

APPLICATION OF THE GREEN FUNCTION METHOD TO THE NUCLEI ^{90}Zr AND ^{86}Kr

WALTER J. MULHALL and ROBERTO J. LIOTTA

Centro Atómico Bariloche
 (C.N.E.A.)

and

Instituto de Física "Dr. J. A. Balseiro"
 (U.N.C. and C.N.E.A).
 San Carlos de Bariloche

Received 27 October 1966

Abstract: The two-particle Green function method in the ladder approximation (LA) is used to study the effects of ground state pair correlation in the low-lying states of ^{90}Zr and ^{86}Kr ; when the nucleus ^{88}Sr is taken as the core. An appreciable effect is found in the 0^+ states. For comparison, shell-model results are quoted. The calculations in the LA account for the binding energies of ^{90}Zr and ^{86}Kr , the energies of the excited 0^+ and 2^+ state and the mean life of the $^2_0^+$ state, in ^{90}Zr .

1. Introduction

The two-particle Green functions $^1) \dagger$ provide information about the systems obtained through adding or subtracting two particles to a reference system or core, of say A particles. The computation of the Green functions for normal spherical nuclear systems in the ladder approximation (LA) amounts to solving an eigenvalue problem as discussed in GFI.

The main feature of the correlation mechanism taken into account in the LA is a coherent contribution of all terms in the matrix element of the "specific" two particle transfer operator $^{\dagger\dagger} P_{\lambda\mu}^+$ (or $P_{\lambda\mu}$), when the matrix element is taken between the core ground state and the lowest energy state, called a "pairing" vibration, of the $(A+2)$ — (or $A-2$) particle system.

In order to discuss the pair correlation effect in a real case, the low-lying states of the nuclei ^{90}Zr and ^{86}Kr are studied in the LA with the nucleus ^{88}Sr taken as the core. The stability of the 50 neutrons and the structure of the proton single-particle states justify considering the nucleus ^{88}Sr as a normal spherical system $^2, 3)$.

The results show that only the 0^+ states have an appreciable pair correlation, while the other states are either shell-model or practically shell-model states. On this basis, attention is focussed on the 0^+ states.

\dagger Hereafter ref. $^1)$ is referred to as GFI.

$\dagger\dagger$ For the definition of the operator $P_{\lambda\mu}^+$, see formula (30) of GFI.

The experimental data needed for the calculations and their latter analysis are collected in sect. 2.

In sect. 3, some spectroscopic hypothesis, the eigenvalue problem and the residual interaction are presented.

For comparison, shell-model results are given in sect. 4.

The results provided by the Green function method are in sect. 5, while in sect. 6 some conclusions are drawn.

2. Experimental data

2.1. ENERGIES

To study the nuclei ^{90}Zr and ^{86}Kr with the Green function method and the nucleus ^{88}Sr as the core, the single-particle states considered to play an important role are the $\frac{3}{2}^+$ and $\frac{1}{2}^-$ above the Fermi sea and $\frac{3}{2}^-$ and $\frac{5}{2}^-$ in the Fermi sea. As the corresponding energies ε_K are renormalized empirically

$$\varepsilon_{K(\pm)} = E_K(A \pm 1) - E_0(A),$$

they are provided by the nuclei ^{89}Y and ^{87}Rb .

The energies ω of the low lying states

$$\omega_{n(\pm)} = E_n(A \pm 2) - E_0(A)$$

of ^{90}Zr and ^{86}Kr and the energies ε_K are listed in table 1. In fig. 1, the pole energies $\pm\omega_{\pm}$ are shown with some transition data.

2.2. THE $^{90}\text{Zr} \rightarrow ^{90}\text{Zr}$ TRANSITION

The electric monopole or E0 transition proceeds by internal conversion with zero units of angular momentum transferred to the ejected electron. For energies greater than $2mc^2$, as for the transition in ^{90}Zr , monopole pair production is the sum of conversion and pair production probabilities

$$W = W_c + W_{\pi} = \left(1 + \frac{L+M}{K}\right) \left(1 + \frac{W_{\pi}}{W_c}\right) W_K, \quad (1)$$

where W_K is the transition probability for conversion of K-electrons. Introducing the experimental values for the ratios 5),

$$\frac{K}{L+M} = 7.06, \quad \frac{W_c}{W_{\pi}} = 2.38, \quad (2)$$

we obtain

$$W = 1.62W_K. \quad (3)$$

The transition probability for conversion of K-electrons may be written as the product of electronic and nuclear factors ⁶⁾

$$W_K = \Omega \rho^2, \quad (4)$$

here

$$\rho = \frac{1}{R^2} \langle f | \sum_p r_p^2 \left(1 - \sigma \left(\frac{r_p}{R} \right)^2 + \dots \right) | i \rangle, \quad (5)$$

where $|i\rangle$ and $|f\rangle$ are the initial and final nuclear states, r_p the position vector of the p th proton and R the nuclear radius.

The mean life of the $^{20+}$ state is

$$\tau = 90 \pm 6 \text{ nsec}, \quad (6)$$

according to Klopper *et al.* ⁷⁾, Alburger ⁷⁾ has found a value consistent with the above.

The value of Ω obtained from fig. 1 of ref. ⁶⁾ for $Z = 40$ and $k = 3.43$ is $\Omega = 2.1$ nsec. Then from the relation $W = 1/\tau$ the value of ρ^2 fitting the experimental datum is

$$\rho_{\text{exp}}^2 = 3.26_{-0.20}^{+0.23} \times 10^{-3}. \quad (7)$$

The theoretical value of ρ is evaluated using the leading term of expression (5), because the value of σ is in the order of 10^{-2} as given by fig. 5 of ref. ⁶⁾.

2.3. THE E2 TRANSITIONS

The mean life of the 2^+ state is not known, but the branching ratio $B(E2; 2^+ \rightarrow ^10^+)/B(E2; 2^+ \rightarrow ^20^+)$ may be discussed. The available data on the intensity of both transitions are ⁸⁾

$$\begin{aligned} I(2^+ \rightarrow ^10^+) &= 0.14, \\ I(2^+ \rightarrow ^20^+) &= (1 \pm 0.3) \times 10^{-4}, \end{aligned} \quad (8)$$

for each disintegrating ^{90}Nb nucleus. From these data, the following results is obtained:

$$\left[\frac{B(E2; 2^+ \rightarrow ^10^+)}{B(E2; 2^+ \rightarrow ^20^+)} \right]_{\text{exp}} = 0.42_{-0.10}^{+0.17}. \quad (9)$$

Since the value of the intensity $I(2^+ \rightarrow ^20^+)$ has been obtained in a rather indirect measurement, it is not a very reliable value.

3. Spectroscopic hypothesis. Residual interaction

To be able to formulate the eigenvalue problem either for shell-model or Green functions, it is necessary to establish some hypothesis concerning the single-particle states and to assume a residual interaction between the nucleons.

The wave functions of the single-particle states are taken as given by a spherical symmetrical harmonic oscillator potential with a spin-orbit term. The correspondence between the single-particle states and the orbitals associated with that Hamiltonian is given in table 2.

TABLE 2

Correspondence between single-particle states and orbitals of the single-particle Hamiltonian

Single-particle state			Quantum numbers {K}		
J	Energy		n	l	j
$\frac{9}{2}^+$	(1) - 6.159		0	4	$\frac{9}{2}$
$\frac{7}{2}^-$	(2) - 7.074		1	1	$\frac{1}{2}$
$\frac{3}{2}^-$	(3) - 10.592		1	1	$\frac{3}{2}$
$\frac{5}{2}^-$	(4) - 10.995		0	3	$\frac{5}{2}$

The size parameter b of the harmonic oscillator well is related to the oscillation frequency ω_0 by $b^2 = \hbar^2/M^*\omega_0$, where the constant M^* is the effective mass of the quasi-particle. The parameter b is evaluated from the consistency relation

$$\langle r^2 \rangle_{\text{av}} = \frac{3}{5}R^2, \quad (10)$$

where $\langle r^2 \rangle_{\text{av}}$ indicates the average mean value of $\sum_p r_p^2$ in the ground state and R the nuclear radius. Taking

$$R = r_0 A^{\frac{1}{3}} \quad (11)$$

and $\langle r^2 \rangle_{\text{av}}$ as given by the uncorrelated ground state, the value of b for the present case is

$$b = 1.75r_0. \quad (12)$$

The ratio between the effective and real mass may be estimated⁹⁾ from

$$\frac{M^*}{M} = \frac{(\hbar c)^2}{E_m M c^2 \left(\frac{b}{r_0}\right)^2} r_0^{-2},$$

where M is the real mass and E_m the energy peak of the electric dipole (E1) gamma ray absorption. For $A \approx 90$, it is $E_m \approx 18$ MeV, then

$$\frac{M^*}{M} = 0.75r_0^{-2} \text{ fm}^2 = \begin{matrix} 0.52 & \text{for } r_0 = 1.2 \text{ fm} \\ 0.38 & \text{for } r_0 = 1.4 \text{ fm.} \end{matrix}$$

The residual interaction between protons ($T = 1$) is assumed to be a finite-range, spin-dependent, central potential of Gaussian shape

$$V(12) = -V_0(P_s + \tau P_t)e^{-(r_{12}/\lambda)^2}, \quad (13)$$

where P_s and P_t are the projectors on the singlet and triplet-spin parts of the two-particle state vectors, τ a parameter giving the mixing and λ the range of the force. The Coulomb interaction is neglected because its matrix elements are small compared to the nuclear ones.

The eigenvalue problem to be diagonalized in the Green function method is (see eqs. (18) and (19) of GFI)

$$\begin{bmatrix} A & C \\ -\tilde{C} & -B \end{bmatrix} \begin{bmatrix} X_+ \\ X_- \end{bmatrix} = \omega \begin{bmatrix} X_+ \\ X_- \end{bmatrix}, \quad (14)$$

where

$$(A)_{ab, cd} = (\varepsilon_{a(+)} + \varepsilon_{b(+)})\delta_{ac}\delta_{bd} + \langle abJ|V|cdJ\rangle,$$

ab, cd all above the Fermi sea

$$(B)_{ab, cd} = (\varepsilon_{a(-)} + \varepsilon_{b(-)})\delta_{ac}\delta_{bd} + \langle abJ|V|cdJ\rangle, \quad (15)$$

ab, cd all in the Fermi sea

$$(C)_{ab, cd} = \langle abJ|V|cdJ\rangle,$$

ab above the Fermi sea and cd in the Fermi sea. The matrix elements are taken between normalized and antisymmetrized states $|ab, J\rangle$.

For calculating the two-body matrix elements, these are expanded in terms of Talmi integrals I_p as follows:

$$\langle ab, J|V|cd, J\rangle = \sum_p C(ab, cd; J, p)I_p. \quad (16)$$

To evaluate the coefficients $C(ab, cd; J, p)$, the transformation brackets of Moshinsky and Brody¹⁰ were used.

For gaussian shape potentials, the Talmi integrals depend on b and λ through the ratio b/λ , in fact

$$I_p = -\frac{V_0}{(1+2(b/\lambda)^2)^{p+\frac{3}{2}}}. \quad (17)$$

The calculations were performed for $\tau = -0.5, 0$ and 0.5 ; $\lambda/b = 1/\sqrt{2}, 1$ and $\sqrt{2}$ and for a range of values of the strength V_0 for each choice of τ and λ/b .

4. Shell model

In the conventional shell model, the matrix C of eq. (14) is considered zero, inert or uncorrelated core and diagonalizes the matrices A and $-B$ for the ^{90}Zr and ^{86}Kr , respectively.

Shell-model calculations were performed for a set of values of the parameters τ , λ/b and V_0 .

The results show that in only two cases are some energies reasonably fitted, both correspond to a value of $\tau = -0.5$ for the mixing parameter. In one of them (case a) only the 0^+ states of ^{90}Zr and the energy difference $\omega_0(A+2) + \omega_0(A-2)$ are rather well adjusted, while in the other (case b) the states of ^{90}Zr are in agreement with the

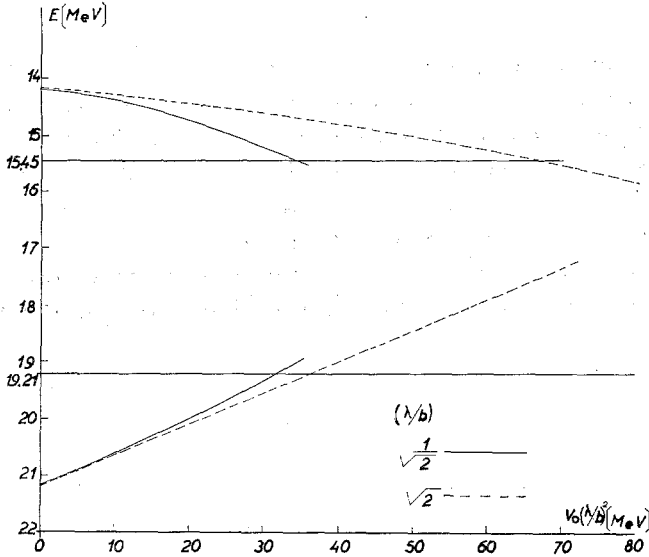


Fig. 2. Shell-model ground states for ^{90}Zr and ^{86}Kr . The horizontal lines indicate the experimental values.

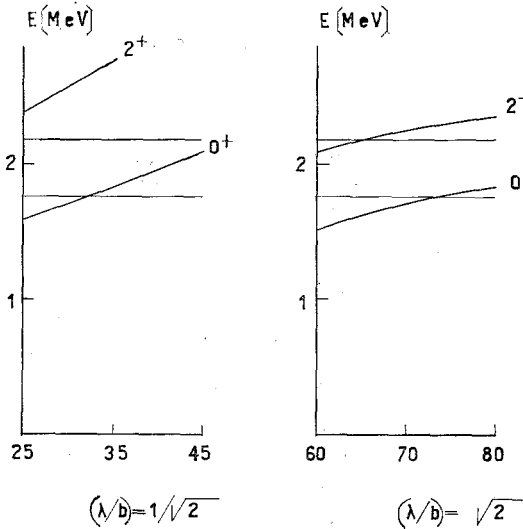


Fig. 3. Excited shell-model states for ^{90}Zr . The horizontal lines indicate the experimental values.

experimental values but the energy difference is not. The values of the parameters for the two cases are

	λ/b	$V_0(\lambda/b)^2$
(a)	$1/\sqrt{2}$	$\approx 32,$
(b)	$\sqrt{2}$	$\approx 70.$

The previous results are displayed in figs. 2 and 3.

It should be noted that in case b), where the levels of ^{90}Zr are suitably adjusted, one may doubt the validity of the shell model. In fact, the binding energy of ^{86}Kr differs from the experimental value and the interaction matrix elements are of the order of the spacing δ between particle and hole levels; $\delta = \epsilon_{2(+)} + \epsilon_{3(-)} \approx 3.5$ MeV and $\langle V \rangle \approx 3.6$ MeV for the state $|p_{\frac{3}{2}} p_{\frac{3}{2}}; 0\rangle$ and $V_0 = 35$ MeV.

To show the structure of the vector states, their energies and corresponding amplitudes $X(ab; nJ)$ are listed in table 3 for values of parameters close to those of cases a) and b).

TABLE 3
The calculated energies and vector amplitudes of the shell-model states for ^{90}Zr and ^{86}Kr

Interaction			State			Amplitudes $X(ab; nJ)$						
τ	λ/b	$V_0(\lambda/b)^2$	Nucleus	J^π	Exc. energy ^{a)}		(11)	(22)	(33)	(34)	(44)	
-0.5	$1/\sqrt{2}$	30	^{90}Zr	10^+	-15.230	0	-0.496	0.868	0	0	0	
				20^+	-13.542	1.69	0.868	0.496	0	0	0	
				2^+	-12.676	2.554	1	0	0	0	0	
			^{86}Kr	0^+	-19.328	0	0	0	0.866	0	0.499	
			35	^{90}Zr	10^+	-15.495	0	-0.557	0.820	0	0	0
					20^+	-13.661	1.83	0.820	0.557	0	0	0
	2^+	-12.735			2.76	1	0	0	0	0		
	^{86}Kr	0^+	-19.030	0	0	0	0.871	0	0.492			
	$\sqrt{2}$	60	^{90}Zr	10^+	-15.268	0	0.400	0.916	0	0	0	
				20^+	-13.751	1.52	0.916	0.499	0	0	0	
				2^+	-13.193	2.07	1	0	0	0	0	
			^{86}Kr	0^+	-17.890	0	0	0	0.966	0	0.258	
70			^{90}Zr	10^+	-15.578	0	-0.515	0.883	0	0	0	
				20^+	-13.866	1.71	0.883	0.515	0	0	0	
		2^+		-13.339	2.24	1	0	0	0	0		
^{86}Kr		0^+	-17.332	0	0	0	0.964	0	0.267			
80		^{90}Zr	10^+	-15.859	0	-0.568	0.823	0	0	0		
			20^+	-14.011	1.85	0.823	0.568	0	0	0		
			2^+	-13.485	2.37	1	0	0	0	0		
^{86}Kr		0^+	-17.686	0	0	0	0.875	0	0.484			

^{a)} In the left column the excitation energies are referred to the energy $E_0(A)$.

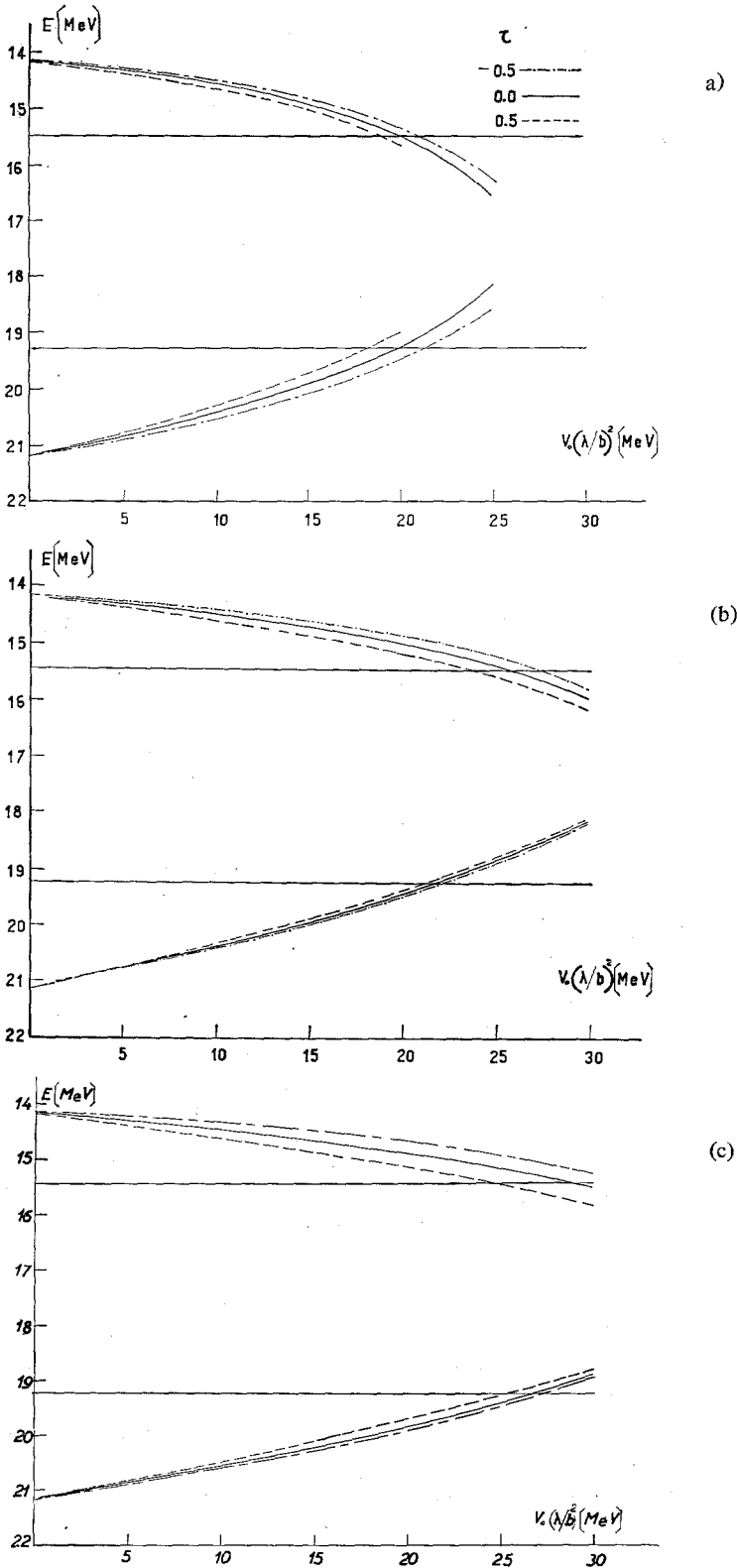


Fig. 4. Ground states of the nuclei ^{90}Zr and ^{86}Kr calculated with the Green function method in the LA. The horizontal lines indicate the experimental values. (a) $\lambda/b = 1/\sqrt{2}$, (b) $\lambda/b = 1$ and (c) $\lambda/b = \sqrt{2}$.

In order to discuss the E0 transition, the strength parameter ρ^2 is evaluated for the states of table 3. From expressions (5) and (11), we obtain

$$\rho^2 = \frac{\langle r \rangle^2}{403 \cdot 326} \left(\frac{b}{r_0} \right)^4, \quad (18)$$

where $\langle r^2 \rangle b^2 = \langle f | \sum_p r_p^2 | i \rangle$. Taking for b/r_0 the value given by eq. (12) the results are as follows:

(a)		(b)	
$V_0(\lambda/b)^2$	ρ^2	$V_0(\lambda/b)^2$	ρ^2
30	1.73×10^{-2}	60	1.71×10^{-2}
35	1.94×10^{-2}	70	2.11×10^{-2}
		80	2.47×10^{-2}

It is observed that the theoretical values are several times larger than the experimental ones.

The corresponding branching ratios (b.r.) $B(E2; 2^+ \rightarrow 10^+)/B(E2; 2^+ \rightarrow 20^+)$ are of the order of the experimental values

(a)		(b)	
$V_0(\lambda/b)^2$	b.r.	$V_0(\lambda/b)^2$	b.r.
30	0.33	60	0.19
35	0.46	70	0.34
		80	0.38

Summing up, the shell model describes the b.r. reasonably well, but it does not fit the energies of all states and the E0 transition probability. It is easily proved that the shell model is not capable of giving the two transition data and the normalization of states when the parameter b/r_0 is given by eq. (12).

5. Green function method

Calculations with the Green function method were also performed for the nine combinations of the parameters τ and λ/b given in sect. 2. The calculated pole energies for the ground states of ^{90}Zr and ^{86}Kr are shown in fig. 4, where it is observed that to a large extent those energies are not sensitive to variations of τ and that several combinations of force parameters fit the energy difference $\omega_0(A+2) + \omega_0(A-2)$ rather well. The ground states show a stronger energy correlation when the force range is smaller, i.e. the value of $V_0(\lambda/b)^2$ fitting the energy difference decreases for smaller values of λ/b .

In fig. 5, the 0^+ and 2^+ states of ^{90}Zr are shown for the different combinations of τ and λ/b and for values of $V_0(\lambda/b)^2$ that reasonably adjust the ground state energies. As can be observed in fig. 5, the energy of the excited 0^+ state is only given for the

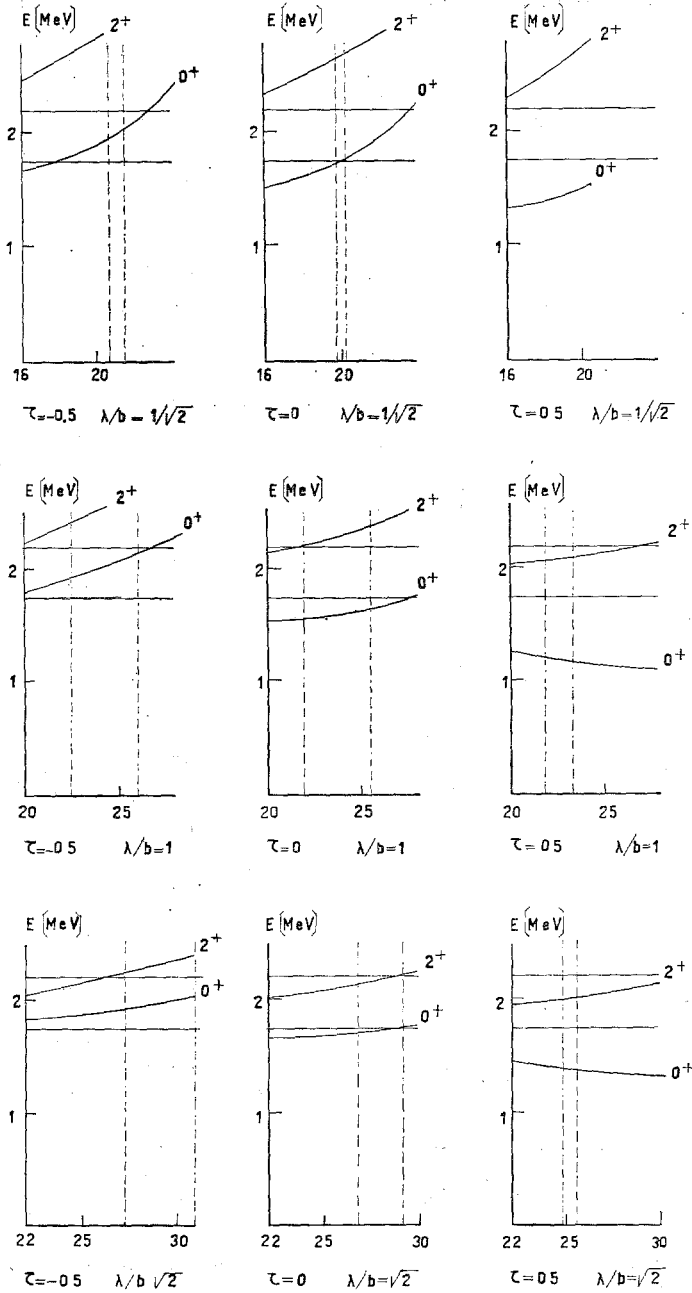


Fig. 5. Excited state of the nucleus ^{90}Zr . The excitation energies are plotted as a function of $V_0(\lambda/b)^2$. The horizontal lines indicate the experimental values.

following values of the parameters:

	τ	λ/b	$V_0(\lambda/b)^2$
(a)	0	$1/\sqrt{2}$	20
(b)	0	$\sqrt{2}$	28.

It is remarkable that, in addition, case (b) also fits the 2^+ state.

TABLE 4

The calculated energies and vector amplitudes of the core pair correlated states for ^{90}Zr and ^{86}Kr

Interaction			State			Amplitude $X(ab; nJ)$						
τ	λ/b	$V_0(\lambda/b)^2$	Nucleus	J^π	Exc. energy ^{a)}	(11)	(22)	(33)	(34)	(44)		
0	$1/\sqrt{2}$	15	^{90}Zr	10^+	-14.919	0	-0.307	0.977	0.221	0	0.012	
				20^+	-13.314	1.60	0.969	0.286	-0.084	0	0.113	
				0^+	-12.679	2.24	1.002	0	-0.014	-0.013	-0.031	
			^{86}Kr	0^+	-19.891	0	0.112	0.191	0.990	0	0.263	
				^{90}Zr	10^+	-15.497	0	-0.502	0.952	0.397	0	0.009
					20^+	-13.767	1.73	0.913	0.447	-0.079	0	0.116
	2^+	-12.819	2.68		1.002	0	-0.015	-0.013	-0.032			
	^{86}Kr	0^+	-19.228	0	-0.204	0.324	1.042	0	0.248			
		^{90}Zr	10^+	-16.561	0	-0.785	1.124	0.938	0	-0.015		
			20^+	-14.039	2.52	0.867	0.550	-0.063	0	0.224		
	2^+		-12.934	3.63	1.002	0	-0.025	-0.025	-0.054			
	^{86}Kr	0^+	-18.132	0	-0.532	0.753	1.350	0	0.166			
^{90}Zr		10^+	-14.901	0	-0.108	1.009	0.171	0	0.021			
		20^+	-13.142	1.76	0.998	0.105	0.019	0	0.085			
	2^+	-12.926	1.98	1.001	0	-0.009	-0.007	-0.047				
^{86}Kr	0^+	-19.813	0	-0.022	0.171	0.999	0	0.178				
	^{90}Zr	10^+	-15.511	0	-0.177	1.047	0.356	0	0.039			
		20^+	-13.648	1.86	0.997	0.168	-0.016	0	0.146			
2^+		-13.248	2.26	1.003		-0.014	-0.012	-0.075				
^{86}Kr	0^+	-18.899	0	-0.047	0.356	1.041	0	0.214				

^{a)} In the left column the excitation energies are referred to the energy $E_0(A)$.

To show how the pair correlation comes in, the energy of the states and the corresponding vector amplitudes $X(ab; nJ)$ are listed in table 4, for parameters in the regions (a) and (b). Measuring the pair correlation for the $(A \pm 2)$ -particle system by

$$\sum_{a \leq b} |X(ab; J^\pi)|^2 \frac{1}{2} [1 \mp (1 - n_a - n_b)], \quad (19)$$

a rather strong correlation is obtained for the 0^+ state as shown in the following table

		pair correlation	
		(a)	(b)
^{90}Zr	10^+	0.16	0.13
	20^+	0.03	0.02,
^{86}Kr	10^+	0.15	0.13
	20^+	0.02	0.02,

while the other states are practically shell model.

The transition matrix elements are evaluated from formula (28) of GFI. For the K-electron conversion, we obtain

$$\langle n0 || M(E0) || n'0 \rangle = 2 \sum_a (1 - 2n_a) X^*(aa, n0) X(aa, n'0) \times \frac{1}{\sqrt{2j_a + 1}} \langle j_a || M(E0) || j_a \rangle, \quad (20)$$

and for the E2 transition

$$\langle n2 || M(E2) || n'0 \rangle = \sqrt{2} \sum_{j_a j_b} (1 - 2n_b) X^*(ab, n2) X(bb, n'0) \times N^{-1}(ab, 2) \frac{1}{\sqrt{2j_a + 1}} \langle j_a || M(E2) || j_b \rangle. \quad (21)$$

The matrix element $\langle r^2 \rangle$ for the different force parameter combinations are shown in fig. 6. From this graph and formula (18), the strength ρ^2 is obtained while the branching ratio is evaluated from eq. (21). The terms contributing to the E2 matrix

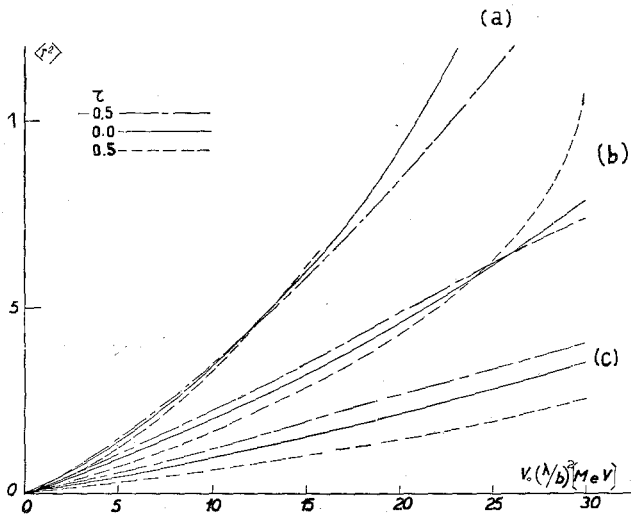


Fig. 6. The matrix element $\langle r^2 \rangle$. (a) $\lambda/b = 1/\sqrt{2}$, (b) $\lambda/b = 1$ and (c) $\lambda/b = \sqrt{2}$.

element show the destructive interference, as remarked in GFI, between those above and in the Fermi sea. Since the 2^+ state is practically shell model, the effect is a minor one.

The resulting values of the transition matrix elements for the cases (a) and (b) are

	ρ^2	b.r.
(a)	1.97×10^{-2}	$ 1.70/3.14 ^2 = 0.29$
(b)	2.38×10^{-3}	$ 0.58/3.45 ^2 = 0.03.$

For case (a) the strength parameter is rather large while the branching ratio, as in the shell model, has a reasonable value. For case (b) the value of ρ^2 adjusts rather well the experimental value, but the branching ratio does not. The difference between the two sets of values is due to the structure of the 0^+ states; in the first case the mixing is favourable for $B(E2; 2^+ \rightarrow 1^0^+)$ but in the second case the value of $B(E2; 2^+ \rightarrow 2^0^+)$ is enhanced over the value corresponding to the transition in the configuration $(\frac{9}{2}^+)^2$.

With respect to the two-particle transfer operators $P_{\lambda\mu}^+(P_{\lambda\mu})$ a coherent contribution of all terms is found for the states of angular momentum λ and lowest energy. No numerical evaluations were performed.

One may conclude by saying that the Green function method has been able to fit with a long-range, singlet-channel force, all the discussed experimental data except the branching ratio.

6. Conclusions

The Green function method introduces the ground state pair correlation through an extended eigenvalue problem and, as a consequence, of this extension the computed eigenvalues are bound to give the binding energies of the systems of $(A \pm 2)$ particles. Conventional shell-model calculations generally ignore this restriction; this may lead to situations where the shell model could have little validity as in case (b) of sect. 4.

The Green function 0^+ states show an appreciable pair correlation and thus behave differently from the corresponding shell-model states. In consequence, the "fitting" force parameters have different values.

The core correlated calculations give a good fitting of the experimental data discussed. The discrepancy in the branching ratios may indicate that particle-hole correlation should be included. In any case the available experimental intensity $I(2^+ \rightarrow 2^0^+)$ needs further confirmation.

It may be added that the model states not discussed in this paper have energies lower than the experimental one. Furthermore, it is worthwhile to note that, as discussed by Bayman *et al.*³⁾, those states do not describe the available transition data. It would appear that new features, such as particle-hole correlations, should be incorporated to the models in order to correct this shortcoming.

The authors wish to thank Dr. J. A. Evans and Dr. D. R. Bes for valuable comments and Dr. R. Ch. de Guber for making computation facilities available at the Instituto de Cálculo de la Universidad de Buenos Aires.

Appendix

For the E0 transition in ^{90}Zr , taking the value of the mean life of the $^{20+}$ state as given by Alburger⁷⁾

$$\tau = 87 \pm 22 \text{ nsec}, \quad (\text{A.1})$$

we obtain

$$\rho^2 = (3.38_{-0.69}^{+1.14}) \times 10^{-3}. \quad (\text{A.2})$$

This value is nearly the same as that given by formula (7) but the error is increased.

To illustrate the sensitivity of the theoretical value of ρ^2 to the variation of V_0 , in the region where the energies are well fitted, the following calculation is made for $\tau = 0$, $\lambda/b = \sqrt{2}$ and $V_0 = 30$:

$$\rho^2 = 2.88 \times 10^{-3}. \quad (\text{A.3})$$

This value coincides with the value (A.2), within the error. (Compare $\rho^2 = 2.38 \times 10^{-3}$ corresponding to $\tau = 0$, $\lambda/b = \sqrt{2}$ and $V_0 = 28$.)

References

- 1) W. J. Mulhall, R. J. Liotta, J. A. Evans and R. P. J. Perazzo, *Nuclear Physics* **A93** (1967) 261
- 2) K. W. Ford, *Phys. Rev.* **98** (1955) 1516
- 3) B. F. Bayman, A. S. Reiner and R. K. Sheline, *Phys. Rev.* **115** (1959) 1627
- 4) J. H. E. Mattauch, W. Thiele and A. H. Wapstra, *Nuclear Physics* **67** (1965) 1
- 5) *Nuclear Data Sheets*, ed. by K. Way *et al.*, National Academy of Science - National Research Council, Washington, D.C.
- 6) E. L. Church and J. Weneser, *Phys. Rev.* **103** (1956) 1035
- 7) R. M. Kloepper, R. B. Day and D. A. Lind, *Phys. Rev.* **114** (1959) 240;
D. E. Alburger, *Phys. Rev.* **109** (1958) 1222
- 8) S. Bjørnholm, O. B. Nielsen and R. K. Sheline, *Phys. Rev.* **115** (1959) 1613
- 9) S. A. Moszkowski, *Encyclopedia of physics*, Vol. **39**, ed. by S. Flügge (Springer-Verlag, Berlin, 1957) p. 469
- 10) T. A. Brody and M. Moshinsky, *Tables of transformation brackets* (Monografías del Instituto de Física, México, 1960)